IR Surface Characterization of Some TiO_2-Based Pigments. 1. Preparation of Pigmentary Materials

C. Morterra* and G. Cerrato

Dipartimento di Chimica Inorganica, Chimica Fisica e Chimica dei Materiali, Università di Torino, via P. Giuria 7, I-10125 Torino, Italy

M. Visca and D. M. Lenti

Montefluos S.p.A., Colloid Laboratory, I-15047 Spinetta Marengo, Italy

Received June 1, 1990. Revised Manuscript Received October 12, 1990

Several preparations of TiO_2 (anatase) containing different additives, bound to play different roles either temporarily during the sintering process or permanently, in the final pigment, have been studied by in situ FTIR spectroscopy. The samples were examined by checking the changes of the background spectra as well as the room-temperature adsorptive properties toward pyridine (py) on varying the oven firing temperature, from the starting gel phase (300 K) to the final pigmentary product stage (1185 K). Up to a firing temperature of ≈1047 K, no appreciable differences can be noted in the behavior of the various preparations, and the gradual spectral changes observed mainly involve the degree of surface hydration and the surface coverage/decomposition of sulfate groups deriving from the preparative process. These two parameters affect the relative importance of the Lewis and Brønsted surface acidity. For firing at $T > 1073$ K, the various preparations start differing appreciably: the elements added to the TiO_2 matrix in the gel precipitation stage tend to segregate (to a variable extent) at the surface of the solid and modify the surface acidic behavior of the sintering pigmentary material.

1. Introduction

Previous work from some of us[1-7] was devoted, over the past 10 years, to the understanding of the surface properties of TiO_2 (anatase), of their dependence on the material preparation route, and of the effects produced by some contaminants and/or additives on the activity of TiO_2 surface centers.

Various surface chemistry procedures were adopted, including an IR study of the adsorption of several probe molecules, in order to reveal the modification of TiO_2 surface activity with thermal activation and other physical and/or chemical treatments.

Many aspects of the surface chemistry of anatase are now understood, and among them it is worthwhile recalling the following: (i) The surface hydrated layer of TiO_2 is made up of surface hydroxyls of more than one type[8,9] and of undissociated molecular water coordinated at coordinatively unsaturated (cus) surface Ti^{4+} centers. The latter are responsible for the strongest surface Lewis acidity, as revealed by the coordinative chemisorption of CO at ambient temperature[3,5-7,10,11] as well as by the adsorption of other Lewis bases. (ii) Surface sulfate groups, either introduced artificially to increase the activity of the solid[12] or deriving from the preparative process,[2,3] modify to an appreciable extent the Lewis acid–base properties of the TiO_2 surface. (iii) Cationic species other than Ti, e.g., K[5] or Na,[10] which can be either introduced in the early stages of the TiO_2 preparation or added by impregnation, collect at the surface during the thermal treatments and modify the termination of the TiO_2 crystallites and the surface Lewis acid–base properties.

It is well-known that TiO_2, in both rutile and anatase modifications, is the basis of the most commonly used white pigments (see ref 13, and references therein). It is also known that to gain adequate pigmentary properties, TiO_2 must undergo several physical and/or chemical treatments of a rather complex nature.

The knowledge of the chemical form and of the localization of impurities and additives during the preparation of a TiO_2-based pigment is thus much more than a mere problem of elemental analysis, and various analytical tools must be resorted to to gain that knowledge.

For this reason it was believed that the investigation of the surface properties of a pigmentary TiO_2 system by standard surface chemistry procedures could be a useful complementary tool to the usual chemical and physical methods of bulk analysis.

Previous experience on various aspects of the surface properties of several oxidic systems (e.g., see ref 14) suggested us that the IR spectroscopic investigation of pyridine (py) adsorption/desorption may be regarded as a convenient analytical tool to check the transformations of the outer layer of TiO_2 particles.

In fact, py adsorption is known to be quite selective in distinguishing among various types of adsorptive activity[15-19] as well as in distinguishing different cus cationic centers acting as Lewis acidic sites.[19-21]

(1) Morterra, C.; Chiorino, A.; Zecchina, A.; Fisicaro, E. *Gazz. Chim. Ital.* **1979**, *109*, 683.
(2) Morterra, C.; Chiorino, A.; Zecchina, A.; Fisicaro, E. *Gazz. Chim. Ital.* **1979**, *109*, 691.
(3) Morterra, C.; Ghiotti, G.; Garrone, E.; Fisicaro, E. *J. Chem. Soc., Faraday Trans. 1* **1980**, *76*, 2102.
(4) Morterra, C.; Chiorino, A.; Boccuzzi, F.; Fisicaro, E. *Z. Phys. Chem. (Munich)* **1981**, *124*, 211.
(5) Morterra, C.; Chiorino, A.; Ghiotti, G.; Fisicaro, E. *J. Chem. Soc., Faraday Trans. 1* **1982**, *78*, 2649.
(6) Morterra, C. *J. Chem. Soc., Faraday Trans. 1* **1988**, *84*, 1617.
(7) Morterra, C.; Bolis, V.; Fisicaro, E. *Colloids Surf.* **1989**, 177.
(8) Tsyganenko, A. A.; Filimonov, V. N. *J. Mol. Struct.* **1973**, 579.
(9) Tanaka, K.; White, J. M. *J. Phys. Chem.* **1982**, *86*, 4708.
(10) Morterra, C.; Garrone, E.; Bolis, V.; Fubini, B. *Spectrochim. Acta* **1987**, *43A*, 1577.
(11) Bolis, V.; Fubini, B.; Garrone, E.; Morterra, C. *J. Chem. Soc., Faraday Trans. 1*, **1989**, *85*, 1383.
(12) Busca, G.; Saussey, H.; Saur, O.; Lavalley, J. C.; Lorenzelli, V. *Appl. Catal.* **1985**, *14*, 245.
(13) Garbassi, F.; Mello Ceresa, E.; Occhiello, E.; Pozzi, L.; Visca, M.; Lenti, D. M. *Langmuir*, **1987**, *3*, 173.
(14) Zecchina, A.; Coluccia, S.; Morterra, C. *Appl. Spectrosc. Rev.* **1985**, *21*, 259.
(15) Parry, E. P. *J. Catal.* **1963**, *2*, 371.
(16) Hughes, T. R.; White, H. M. *J. Phys. Chem.* **1967**, *71*, 2192.
(17) Pichat, P.; Mathieu, M. V.; Imelik, B. *Bull. Soc. Chim. Fr.* **1969**, *8*, 2611.
(18) Scokart, P. O.; Declerck, F. D.; Sempels, R. E. *J. Chem. Soc., Faraday Trans. 1* **1977**, *73*, 359.
(19) Connell, G.; Dumesic, J. A. *J. Catal.* **1987**, *105*, 285.
(20) Ward, J. W. *J. Catal.* **1968**, *10*, 34.
(21) Ratov, A. N.; Kubasov, A. A.; Topchieva, K. V.; Rosolovskaya, E. N.; Kalinin, V. P. *Kinet. Catal.* **1973**, *14*, 896.

0897-4756/91/2803-0132$02.50/0

The present contribution deals with the surface transformations undergone by several TiO_2-based pigmentary materials during the firing treatments which bring the starting gel phase to the last calcining stage. The latter yields the so-called "final product".

2. Experimental Section

2.1. Materials. Three TiO_2 pigmentary specimens, listed below, were prepared by SIBIT S.p.A., Milano, through the via-sulfate process. The preparation was carried out on a laboratory scale, reproducing with reagents of the highest purity the procedures of the industrial plant. Starting material was in all cases pure titanyl sulfate, hydrolyzed with H_2SO_4 in the presence of dosed amounts of the selected additives. Abundant residual sulfates, deriving from the preparation process, are thus the only contaminants, whereas all other foreign elements were deliberately added by gel precipitation and dosed in the dried gel by standard analytical methods.

TSK: This is the standard pigmentary preparation. In the starting gel phase the amount of residual S (measured as SO_3) is ≈3%. It contains the following additives: P_2O_5, 0.15%; K_2O, 0.2%; rutile active seed (ras), 3%.

TSZ: This is a preparation photostabilized with Zn. It contains the following: residual S, ≈3%; P_2O_5, 0.15%; K_2O, 0.18%; ZnO, 0.25%; ras, 3%.

TSA: This is a preparation photostabilized with Al. It contains the following: residual S, ≈3%; P_2O_5, 0.15%; K_2O, 0.2%; Al_2O_3, 0.15%; ras, 3%.

Other samples of simpler and controlled composition have been used as reference materials for the IR assignments:

TSS: This is the standard via-sulfate anatase preparation with no additives (i.e., free from foreign cations). It contains, in the starting gel phase, ≈3% of residual S (measured as SO_3).

TS: This is pure anatase free from both cationic and anionic impurities; BET sa 83 $m^2\ g^{-1}$.

TCZ: This is an anatase preparation loaded, by impregnation, with 1% Zn (from Zn acetate); BET sa 48 $m^2\ g^{-1}$ at (up to) 873 K, ≈7 $m^2\ g^{-1}$ at 1100 K.

TCP: This is an anatase preparation loaded, by impregnation, with 0.2% P_2O_5; BET sa ≈6 $m^2\ g^{-1}$ at 1100 K.

TCPK: This is an anatase preparation loaded, by impregnation, with 0.2% P_2O_5 and 0.2% K_2O; BET sa ≈6 $m^2\ g^{-1}$ at 1100 K.

ZnO: This is pure ZnO (Kadox 25, New Jersey Zinc Co., BET sa 11 m^2/g^{-1}).

AlO(θ): This was pure θ-Al_2O_3 prepared by firing η-Al_2O_3 at 1095 K for 22 h; BET sa ≈75 $m^2\ g^{-1}$.

2.2. Terminology. Samples of the pigmentary TiO_2 specimens were taken from the laboratory rotary furnace after firing at various temperatures between the initial gel stage and the final product stage and were investigated separately.

The sample *sintering stage*, i.e., the highest temperature (kelvin) reached by the materials in the furnace is indicated in the text and figures as a numeral, subscript to the symbol of the specimen (e.g., TSZ_{673} stands for a sample of the TSZ preparation extracted from the furnace after reaching a firing temperature of 673 K). Samples of the starting gels dried in air at ambient temperature do not carry any subscript.

The sample *activation stage*, i.e., the temperatures (kelvin) at which the samples were treated in the vacuum system prior to adsorption experiments are indicated in the text and figures as a numeral following the symbol of the specimen (e.g., $TSK_{873}673$ stands for a sample of the TSK preparation, taken from the furnace after reaching 873 K, prepared in the form suitable for IR measurements, and activated in vacuo at 673 K for some 2 h).

2.3. Methods. Most of the materials here investigated, and especially those corresponding to advanced stages of the preparation, possess very poor cohesion and are so opaque, due to severe light-scattering losses, that no self-supporting pellets of the type normally employed in surface chemistry could be used for the IR measurements.

IR samples were then prepared in the form of thin layers (4–12 mg cm^{-2}), deposited from an isopropyl alcohol suspension over a pure Si plate. The wafers were transferred to the vacuum system (residual pressure $<10^{-5}$ Torr), where they underwent all thermal and spectroscopic treatments without any further exposure to the atmosphere.

IR spectra were run at 4-cm^{-1} resolution on a FTIR spectrometer Bruker 113v equipped with a DTGS detector. A large number of scans (normally 256) was accumulated for each spectrum, in order to bring the signal-to-noise ratio to an acceptable level. All adsorption measurements were carried out in a strictly in situ configuration, so that the spectra ratioing and background subtractions could be performed routinely, to lend the resulting spectra a quasi-quantitative meaning.

Whenever needed, segments of the spectra of adsorbed py were band-resolved by using an iterative Pascal program by Bruker, which fixes only the number of spectral components to be resolved and the accuracy level desired, whereas all other parameters ($\tilde{\nu}_{max}$, $\Delta\tilde{\nu}_{1/2}$, percent Gaussian, etc.) are allowed to float freely.

3. Results and Discussion

The preparation of a TiO_2-based pigment implies the stepwise thermal treatment of a starting precipitate in the temperature range 300–1185 K.

For the sake of clarity, the overall firing temperature interval will be split in two subranges, as in them rather different transformations occur on the pigmentary materials.

For each temperature subrange, the spectral changes brought about by the firing process will be presented first. Then, the adsorptive interaction with py will be examined, to check the surface transformations produced in each calcining/activation step.

3.1. Thermal Treatments at Temperatures up to 1073 K. 3.1.1. Effect of the Thermal Treatments (Background Spectra). In the temperature interval 300–1073 K the surface area of TiO_2 declines from ≈230 to ≈25 $m^2\ g^{-1}$, with no appreciable differences among the three pigmentary preparations examined. Curve a of Figure 1A reports the surface area of the TSZ preparation as a function of the firing temperature.

In the same temperature interval sulfate contaminants, deriving from the preparative process, are progressively eliminated. Figure 2, relative to TSS (reference preparation), and Figure 3, relative to TSZ (in this temperature interval no appreciable differences were observed between TSK, TSA, and TSZ, and only the latter preparation will be presented in detail), indicate that the presence of sulfate species is easily recognizable in the IR spectra. On hydrated samples (curve a of Figure 2, and curves a, b, e of Figure 3) there are some broadish bands, progressively less defined with increasing firing temperature, at $\tilde{\nu} < 1350$ cm^{-1}, whereas in the case of dehydrated samples (curve b in Figure 2, and curves c and f in Figure 3) characteristic sharp bands can be observed in the 1400–1300-cm^{-1} range. On sulfate-free preparations treated at $T \leq 1073$ K (see curve e in Figure 2, relative to TS) the whole 1500–850-cm^{-1} range is free from absorptions.

The mentioned bands, previously assigned for other TiO_2 preparations,[2,5] are due to sulfates in systems with different conditions of hydration and surface polarity and are quite common on various sulfate-doped oxidic materials.[22-25]

The sharp bands observed at 1400–1300 cm^{-1} for dehydrated samples are a convenient monitor of the surface fraction of sulfate contaminants. They correspond to the asymmetric S=O stretching vibrations of highly covalent

(22) Saur, O.; Bensitel, M.; Mohammed Saad, A. B.; Lavalley, J. C.; Tripp, C. P.; Morrow, B. A. *J. Catal.* **1986**, *99*, 104.
(23) Yamaguchi, T.; Jin, T.; Tanabe, K. *J. Phys. Chem.* **1986**, *90*, 3148.
(24) Morrow, B. A.; McFarlaine, R. A.; Lion, M.; Lavalley, J. C. *J. Catal.* **1987**, *107*, 232.
(25) Bensitel, M.; Saur, O.; Lavalley, J. C.; Morrow, B. A. *Mater. Chem. Phys.* **1988**, *19*, 147.

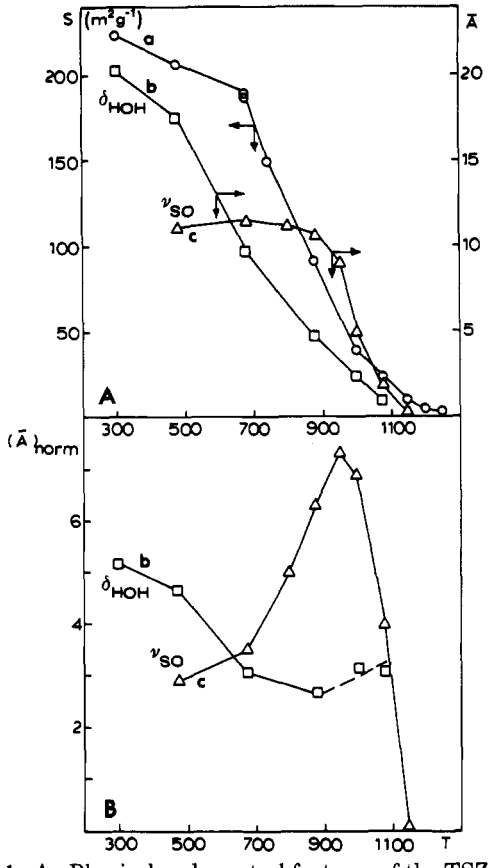

Figure 1. A: Physical and spectral features of the TSZ preparation. Changes with oven firing temperature of the specific surface area S (curve a) and of the integrated absorbance Ā of the δ_{HOH} mode (curve b, samples TSZ_T300) and of the ν_{SO} mode (curve c, samples TSZ_T673) (left-hand plot, $m^2\ g^{-1}$ vs K; right-hand plot, cm^{-1} vs K). B: Spectral features of the TSZ preparation. Changes with oven firing temperature of the normalized integrated absorbance $[\bar{A}]_{norm}$ of the δ_{HOH} mode (curve b, samples TSZ_T300) and of the ν_{SO} mode (curve c, samples TSZ_T673) ($cm^{-1}\ m^{-2}\ g^{-1}$ vs K).

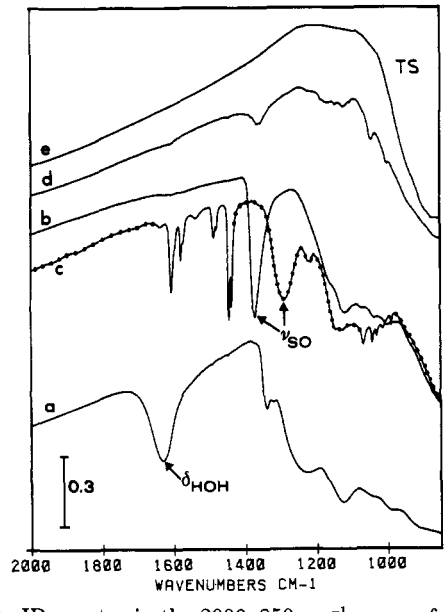

Figure 2. IR spectra in the 2000–850-cm^{-1} range of some TSS and related samples: (a) TSS 300; (b) $TSS_{673}673$ (c) (dotted line) $TSS_{673}673$, in contact with ≈6 Torr of py; (d) $TSS_{873}673$; (e) the reference sample $TS_{873}673$ (transmittance vs wavenumbers).

SO_n groups[26] located at the surface: in fact they are reversibly shifted by the adsorption of charge-releasing

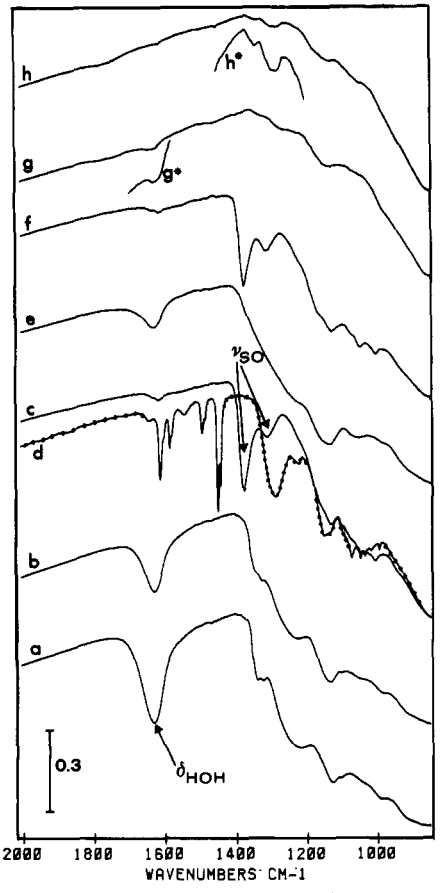

Figure 3. IR spectra in the 2000–850-cm^{-1} range of some TSZ samples: (a) TSZ 300; (b) $TSZ_{673}300$; (c) $TSZ_{673}673$; (d) (dotted line) $TSZ_{673}673$, in contact with ≈6 Torr of py; (e) $TSZ_{873}300$; (f) $TSZ_{873}673$; (g) $TSZ_{1073}300$; (g*) a blown-up segment of curve g in the δ_{HOH} mode range; (h) $TSZ_{1073}673$; (h*) a blown-up segment of curve h in the ν_{SO} mode range (transmittance vs wavenumbers).

and/or polar absorbates. (For the effect of py adsorption, see spectra b and c in Figure 2 and c and d in Figure 3.)

The spectral trends shown in Figures 2 and 3 yield information on the sintering materials, which can be schematically summarized as follows:

(i) On the reference TSS preparation there is a single sharp band at ≈1375 cm^{-1} due to covalent surface sulfates (it is shown by the arrow in Figure 2, curve b). The surface sulfates decline fast at 870 K, yielding a residual band (curve d in Figure 2) somewhat broader and located at slightly lower frequency, and no sulfates ramain at $T \geq 970$ K.

(ii) On hydrated TSZ samples there are little differences, if any, in respect of TSS, whereas on dehydrated TSZ samples evidence is found for the existence of *two* covalent surface sulfates. The relevant S=O stretching modes, shown by the arrows in Figure 3, curve c, absorb at ≈1375 and ≈1306 cm^{-1}, respectively.

The latter band is observed with similar features also on TSK and TSA and is assigned to sulfates involving surface K atoms, as discussed in a previous paper dealing with K_2O-doped anatase.[5] This observation yields indirect evidence for the presence of K atoms at the surface of K_2O-containing TiO_2 preparations, already in the earliest stages of the sintering process.

(iii) With increasing firing temperature, the decreasing surface area of TSZ (curve a of Figure 1A) is somehow

(26) Preud'homme, J.; Lamotte, J.; Janin, A.; Lavalley, J. C. *Bull. Soc. Chim. Fr.* **1981**, *11–12*, I-433.

paralleled, in the hydrated samples, by the decline of a band at ≈1630 cm^{-1}, due to the δ_{HOH} mode of undissociated water molecules[27] coordinated to surface cus cations. For the TSZ_T300 samples this is shown by curve b of Figure 1A.

Still, curve b of Figure 1B, where the absorbance of the δ_{HOH} mode is normalized vs the decreasing surface area and the sample weight, indicates that the amount of coordinated water per unit surface area does not remain constant. Within a firing temperature of ≈900 K it declines by some 40%, whereas for firing temperatures above 900 K it is difficult to say if the specific amount of coordinated water varies any further, due to the weakness of the relevant band for materials of low surface area.

Unlike the δ_{HOH} band, the intensity of the ν_{SO} band of covalent sulfates at the surface of dehydrated materials does not follow the trend of the declining surface area. Curve c of Figure 1A, relative to the TSZ_T673 samples, shows that the relative intensity of the band grows with firing temperature up to ≈900 K and declines afterward, to be eliminated at $T \geq 1173$ K. This trend is shown even more clearly by curve c in Figure 1B, where the intensity of the ν_{SO} band of TSZ_T673 samples is normalized vs the decreasing surface area.

These observations indicate that, during the early stages of the thermal treatment and up to ≈900 K, there is a migration of sulfates from the bulk of the material and that their accumulation at the surface of the crystallites is faster than their surface decomposition. This agrees with previous XPS data.[13]

Previous work[6] showed that the creation of a sulfate layer at the surface of anatase involves quantitatively the particle terminations (i.e., crystal planes and/or coordinative configurations) which, when hydrated, carry hydroxyl groups. The data presented in Figure 1B indicate that the building up of a more and more abundant surface sulfate layer involves also an appreciable fraction (up to ≈40%) of the surface cationic centers which, when hydrated, coordinate undissociated water molecules.

(iv) The relative intensity of the band at ≈1306 cm^{-1}, due to K-related sulfates, grows with firing temperature with respect to the band at 1375 cm^{-1}, due to Ti-related sulfates, and on the sample treated at 1073 K (curve h of Figure 3) it becomes >1. This implies a different rate of decomposition of the two sulfate species and/or a tendency to the segregation of K ions at the surface of a progressively sintered material. This was previously postulated[5,13] and will be demonstrated later.

(v) Curve h of Figure 3 ($TSZ_{1073}673$) shows that, on samples treated at high temperatures, the small residual sulfate bands are shifted to lower wavenumbers, even more than they are on TSS. This indicates that, with temperature, there is a progressive change of the dielectric properties at the surface of the sintering material and that this change is "felt" by the ν_{SO} modes of sulfates.

3.1.2. Adsorption of Py. No data relative to the TSS/py system are reported here. In fact, up to a firing temperature of ≈900 K, the adsorptive behaviour of the reference TSS system is similar to that of TSZ (and similar preparations), and the only differences remain in the nature of sulfates, dealt with in the previous section.

A. Some Features of the Py Spectra. Figure 4 reports segments of the absorbance spectra of py adsorbed on some TSZ samples. Before discussion of the data therein, some of the characteristics of those py spectra ought to be described:

(27) Nakamoto, K. In *Infrared and Raman Spectra of Inorganic and Coordination Compounds*, 4th ed.; Wiley: New York, 1986.

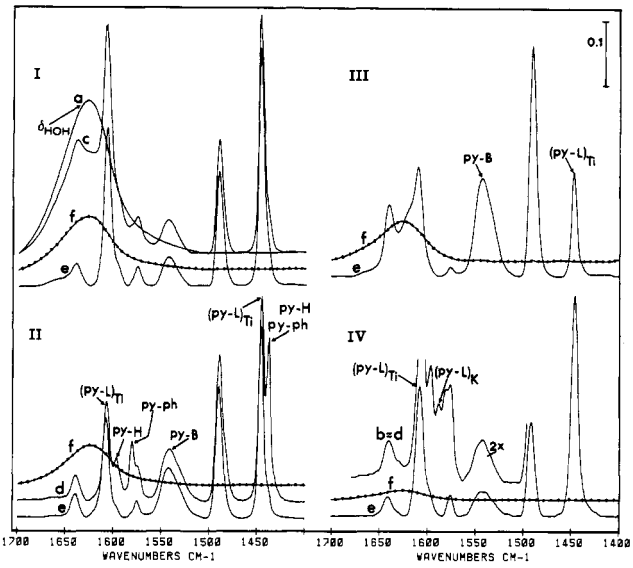

Figure 4. IR spectra in the 1700–1400-cm^{-1} range relative to the interaction of py with some TSZ samples: set I, TSZ300; set II, $TSZ_{673}300$; set III, $TSZ_{873}300$; set IV, $TSZ_{1073}300$. Wherever reported, the curves marked with the letters a–f are (a) the background spectrum, before py uptake; (b) the spectrum after addition of ≈6 Torr of py; (c) the spectrum after py evacuation at ambient temperature; (d) the spectrum recorded in the presence of ≈6 Torr of py (curves b), after band subtraction of the residual spectral contribution of the δ_{HOH} band; (e) the spectrum recorded after py evacuation at ambient temperature (curves c), after band subtraction of the residual spectral contribution of the δ_{HOH} band; (f) (dotted line) the δ_{HOH} spectral component that was eliminated, by ligand displacement, upon py adsorption (absorbance units vs wavenumbers). Symbols: py–ph, physically adsorbed pyridine; py–H, H-bonded py; py–B, py adsorbed in the Brønsted mode; $(py-L)_{Ti}$, py Lewis coordinated to cus Ti^{4+} centers: $(py-L)_K$, py Lewis coordinated to cus K^+ centers.

i. Assignment: The spectra of adsorbed py will be dealt with in this and in the following sections with reference to the nomenclature first adopted by Parry[15] and based on the assignments proposed long before for liquid py and py coordinated in homogeneous phases.[28-30]

ii. Intensity of py bands: Figure 4 reports the spectra of py in the analytical range of the 8a–8b and 19a–19b ring stretching modes.[28,31] The samples were isolated in some significant stages of the oven thermal treatment and were vacuum activated at ambient temperature (they were thus in a highly hydrated state). The absorbance ordinate scale of Figure 4 was normalized vs the sample weight and surface area, in order to give to the relative intensities some quantitative meaning.

iii. Py adspecies and coverage: For some of the samples ($TSZ_{673}300$, curves II, and $TSZ_{1073}300$, curves IV) Figure 4 reports the spectra run both in the presence of a py pressure (≈6 Torr, curves d) and after py evacuation at ambient temperature (curves e). On the former sample, all chemisorbed species are nonreversible and the spectra obtained after py evacuation are sufficient for the present discussion. The latter spectra look obviously simpler, due to the removal of the H-bonded py phase (py-H band at ≈1597 cm^{-1} [15]) and of the liquidlike py phase (py-ph, bands at ≈1580 and ≈1438 cm^{-1} [17]). But for firing temperatures ≥1000 K the spectra are more complex: some chemisorbed

(28) Kline, C. H.; Turkevich, J. *J. Chem. Phys.* **1944**, *12*, 300.
(29) Wilmshurst, J. K.; Bernstein, H. J. *Can. J. Chem.* **1957**, *35*, 1185.
(30) Gill, N. S.; Nuttall, R. H.; Scaife, D. E.; Sharp, D. W. A. *J. Inorg. Nucl. Chem.* **1961**, *18*, 79.
(31) Colthup, N. B.; Daly, L. H.; Wiberley, S. E. In *Introduction to Infrared and Raman Spectroscopy*; Academic Press: New York, 1964; p 225.

py species form, which are partly reversible on evacuation at ambient temperature (see, for instance, the weak band marked $(py\text{-}L)_K$ in the expanded segment of curve IVb and absent in curve IVe), and to observe them, one must consider also the spectra obtained in the presence of a py pressure.

iv. Py uptake and coordinated H_2O: For TSZ 300 (curves I), Figure 4 shows the background spectrum before py adsorption (curve a, dominated by the δ_{HOH} mode of coordinated water at $\approx$1630 cm^{-1}), and the spectrum obtained after py adsorption and subsequent evacuation at ambient temperature (curve c). Upon py adsorption, part of the abundant molecular water coordinated at surface cus Ti^{4+} centers was eliminated through a ligand-displacement mechanism. Curve e is the actual spectrum due to adsorbed py and was obtained from curve c by an interactive band subtraction procedure:

$$e = c - xa$$

where $xa = c - e$ represents the fraction of the original δ_{HOH} band of coordinated water that remained adsorbed at cus Ti^{4+} centers also in the presence of adsorbed py. Curve f, reported as a dotted line, is

$$f = a - (c - e) = (1 - x)a$$

and represents the fraction of the background δ_{HOH} band of coordinated water removed, upon py adsorption by the ligand-displacement mechanism. On TSZ300 the latter component accounts for some 35–40% of the starting intensity of the δ_{HOH} band. A similar figure was also found for each of the TSZ samples treated at higher temperatures, and for them Figure 4 reports the actual spectrum of chemisorbed py (curves e), obtained by band subtraction, and the component of the initial band of coordinated water removed by ligand displacement upon py uptake (curves f).

B. Py Adsorption and Surface Acidity. The detailed spectral investigation of the TSZ/py system, some aspects of which are reported in Figure 4, allows us to observe the following:

(i) On all TSZ_T300 samples there is a py adspecies Lewis coordinated at cus Ti^{4+} surface centers. This species, hereafter referred to in the text and figures as $(py\text{–}L)_{Ti}$, has in the 1700–1400-cm^{-1} range the following analytical modes: 8a, $\approx$1607; 8b, 1575; 19a, $\approx$1490; 19b, $\approx$1445 cm^{-1}. On the basis of literature data,[5,15,30–32] the assignment to Lewis coordination is straightforward.

The formation on TSZ_T300 samples of some cus Ti^{4+} Lewis acidic centers capable of coordinating py is due to a partial dehydration (i.e., the removal of some coordinated water upon mere activation at ambient temperature) and, more than that, to the ligand displacement of some 35–40% of Lewis coordinated water by the adsorbing py, as mentioned above.

The amount of $(py\text{–}L)_{Ti}$ that forms upon py adsorption at ambient temperature can be measured by the integrated absorbance of the $(19b)_L$ mode at $\approx$1445 cm^{-1}. For TSZ_T300 samples this figure is reported, as a function of firing temperature, in Figure 5A, curve a.

Consistent with the changes of concentration of coordinated molecular water (curve b of Figure 1B), the amount of $(py\text{–}L)_{Ti}$ decreases sharply with firing temperature up to $\approx$900 K and then grows again. This trend is a consequence of the postulated segregation at the surface of sulfates, with subsequent coordinative saturation by sulfates of sites capable of coordinating water, followed, for firing at $T \geq 900$ K, by sulfate decomposition (curve c in Figure 1B).

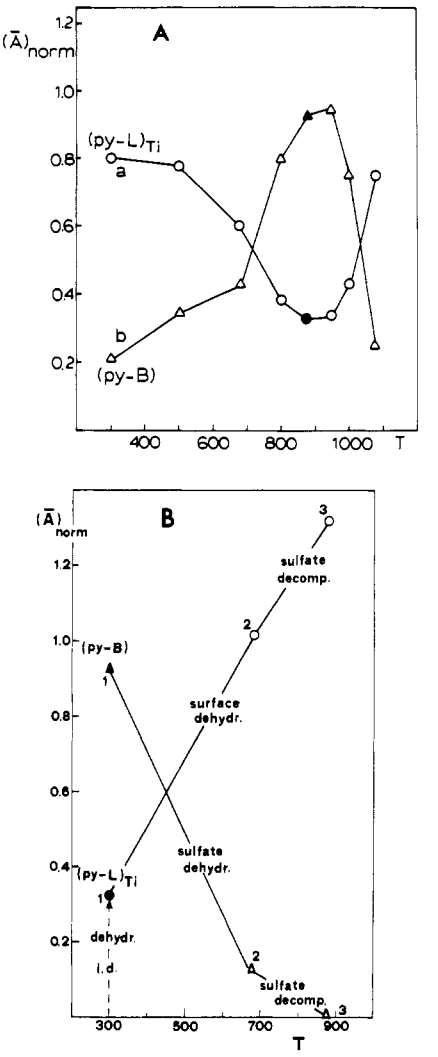

Figure 5. A: TSZ_T300 samples. Changes with oven firing temperature of the specific Ti^{4+} Lewis activity (curve a, normalized integrated absorbance of the $(19b)_L$ mode at $\approx$1445 cm^{-1} vs K) and of the specific Brønsted activity (curve b, normalized integrated absorbance of the $(19b)_B$ mode at $\approx$1540 cm^{-1} vs K). The two experimental points relative to T = 873 K are marked differently (full points), to indicate that they are the same points marked similarly in Figure 5B, and corresponding to the starting points in the plots therein. B: $TSZ_{873}T$ samples. Changes with vacuum activation temperature of the amount of py Lewis coordinated at Ti^{4+} centers (curve a, normalized integrated absorbance of the $(19b)_L$ mode at $\approx$1445 cm^{-1} vs K) and adsorbed in the Brønsted mode (curve b, normalized integrated absorbance of the $(19b)_B$ mode at $\approx$1540 cm^{-1} vs K). For the experimental points 1, marked with different symbols (full point), see the comments in the legend to Figure 5A.

(ii) On TSZ_T300 samples there is also the formation of some py species adsorbed in the Brønsted mode (i.e., in the form of pyridinium ions).

The Brønsted by adspecies, hereafter referred to in text and figures as (py–B), has in the 1700–1400-cm^{-1} range the following analytical modes: 8a, $\approx$1640; 8b, $\approx$1610; 19b, $\approx$1542; 19a, 1490 cm^{-1}. Also this assignment is straightforward on the basis of literature data.[5,15,30–33]

No Brønsted acidity is ever exhibityed by pure TiO_2 preparations. Thus the formation of (py–B) species on highly hydrated sulfate-containing TiO_2 is thought to be due to the presence of some strongly acidic OH groups,

(32) Defossé, C.; Scokart, P. O.; Rouxhet, P. G. *Verres Refract.* **1981**, *35*, 50.
(33) Glazunov, V. P.; Odinokov, S. E. *Spectrochim. Acta* **1982**, *38A*, 399.

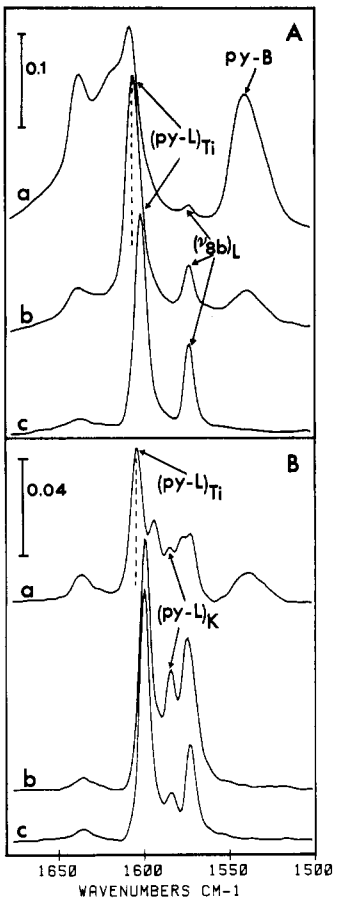

Figure 6. Changes produced by vacuum activation treatments in the spectrum of py adsorbed on some TSZ samples. Section A: $TSZ_{873}T$ samples, after py adsorption and evacuation at ambient temperature. (a) $TSZ_{873}300$; (b) $TSZ_{873}673$; (c) $TSZ_{873}873$. Section B: $TSZ_{1073}T$ samples. (a) $TSZ_{1073}300$, after py uptake (≈6 Torr); (b) $TSZ_{1073}873$, after py uptake (≈6 Torr); (c) as curve b, after py evacuation at ambient temperature (absorbance units vs wavenumbers).

either close to or, more likely, carried by the surface sulfates.[22]

The trend with firing temperature exhibited by the concentration of surface sulfates (curve b of Figure 1B) is closely paralleled by the concentration of the (py–B) species, described by the integrated absorbance of the $(19b)_B$ mode at ≈1540 cm^{-1}. For the TSZ_T300 samples, this is shown by curve b in Figure 5A.

(iii) Besides the firing temperature, also the activation temperature affects the relative concentration of the $(py–L)_{Ti}$ and (py–B) species: upon vacuum thermal treatment, the py Brønsted activity of sulfate-containing TiO_2 specimens declines fast, whereas the Lewis activity increases. For $TSZ_{873}T$ samples, this trend is clearly shown by the plots in Figure 5B and the spectra in Figure 6A. In the latter, the amount of $(py–L)_{Ti}$ is monitored by the 8b mode at ≈1575 cm^{-1}: in fact on these samples $(py–L)_{Ti}$ is still the only species absorbing at that frequency.

The concentration of $(py–L)_{Ti}$ species grows on passing from TSZ300 to $TSZ_{873}673$, as shown by curves a and b in Figure 6A and the relevant points 1 and 2 in Figure 5B. This is ascribable to the vacuum thermal elimination of the residual amount of molecular water coordinated at cus Ti^{4+} centers, which renders available for py coordination more Lewis acidic sites. This process is indicated in Figure 5B as "surface dehydration".

For activation in the same temperature range the concentration of (py–B) decreases, as shown by curves a and b of Figure 6A and the relevant points 1 and 2 in Figrue 5B. The decrease cannot be ascribed to the elimination of surface sulfates, as sulfates do not decompose in vacuo to any appreciable extent at $T < 800$ K. It must be thus ascribed to the thermal elimination of some of the OH groups, most likely carried by surface sulfates, possessing a strong acidic character. This process is indicated in figure 5B as "sulfate dehydration".

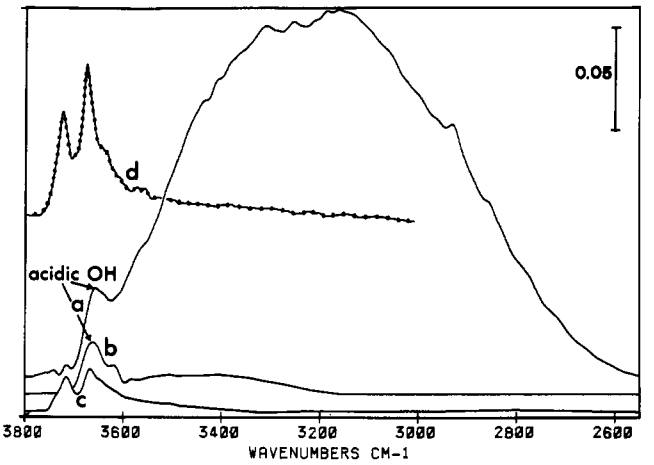

Figure 7. IR spectra in the ν_{OH} region of some $TSZ_{873}T$ and related samples. (a) $TSZ_{873}300$; (b) $TSZ_{873}673$; (c) $TSZ_{873}873$; (d, dotted line) $TS_{723}673$ (absorbance units vs wavenumbers).

The vacuum thermal dehydration of a $TSZ_{870}T$ sample is shown in Figure 7: in the temperature interval 300–673 K (curves a, b) most of the broad and ill-defined band at 3600–2500 cm^{-1}, mainly due to H-bonded coordinated water, is eliminated, and also the band of "free" OH groups at ≈3670 cm^{-1} declines somewhat. The latter band is different from the "free" OH band(s) normally observed on sulfate-free anatase (see curve d and refs 8 and 9) and is ascribed to sulfate-related acidic OH groups.[22] The vacuum thermal elimination of the acidic OH groups absorbing at ≈3670 cm^{-1}, indicated as "sulfate dehydration" in Figure 5B, is responsible for the decrease of Brønsted activity observed in Figure 6A.

The decomposition of sulfates begins at $T \geq 873$ K (curve c of Figure 7), and the spectrum of the (few) residual OH species becomes similar to that normally observed on sulfate-free TiO_2 (spectrum d in the upper part of Figure 7).

Surface and/or sulfate dehydration, two processes occurring in vacuo within ≈673 K, are responsible for the dramatic upward shift of the ν_{SO} bands observed on dehydrated samples and shown in Figures 2 and 3.

The decomposition of sulfates (activation at $T > 800$ K; note that in vacuo the thermal collapse of surface sulfates occurs at lower temperature than in air) brings about a further increase of the $(py–L)_{Ti}$ activity, as shown by curve c of Figure 6A and the relevant points 2 and 3 in Figure 5B. The increased Lewis activity of cus Ti^{4+} centers cannot be ascribed any longer to the elimination of coordinated water, as all of that species was desorbed at lower temperatures. It must be thus related to the gradual removal of the coordinative saturation produced on Ti^{4+} surface centers by sulfates accumulated at the surface.

The decomposition of sulfates is also responsible for the disappearance of (py–B) activity for activation at $T \geq 800$ K. Besides, it causes a downward shift of ≈5 cm^{-1} in the 8a mode of $(py–L)_{Ti}$ (e.g., see spectra b and c in Figure 6A), due to a decreased inductive effect from the charge-withdrawing sulfate groups. In fact, when present, sulfates allow a stronger charge release from the N lone pair of adsorbed py to the Lewis coordinating centers.

(iv) As anticipated above, spectrum b of the set IV in Figure 4 shows that, in the presence of a py pressure, a new weak spectral component appears at ≈1588 cm^{-1} on $TSZ_{1073}300$. The band is fast eliminated upon evacuation at ambient temperature. Curves b and c in Figure 6B indicate that, further to sample activation at $T \geq 670$ K, the new py adspecies grows and becomes partly resistant to py evacuation.

On the basis of previous data[5,20] the assignment of this new spectral component is quite straightforward: it is the 8a mode of py Lewis coordinated to "soft" surface acidic centers and namely to cus K^+ surface ions. The latter are acidic sites weaker than cus Ti^{4+}, owing to the charge and ionic radius, and their weakness is demonstrated by the smaller upward shift of the 8a mode of adsorbed py with respect to unperturbed py.

This species is hereafter referred to in the text and figures as $(py-L)_K$. Its analytical modes in the 1700–1400-cm^{-1} range are as follows: 8a, ≈1588; 8b, 1577 (superimposed with the 8b mode of all py adspecies, except py–B); 19a, ≈1484; 19b, ≈1438 cm^{-1}. Note that the last two modes of the chemisorbed $(py-L)_K$ species (not shown in Figure 6A) virtually coincide with the corresponding modes of other py species weakly held on TiO_2, like H-bonded (py–H, 8a mode at ≈1598 cm^{-1}) and liquidlike physisorbed py (py–ph, 8a mode at ≈1580 cm^{-1}).

The presence of some K^+ ions at the surface of TSZ (as well as of other K-containing preparations) was postulated above on the basis of the spectral features of surface sulfates, which showed two peaks at $\tilde{\nu} > 1300$ cm^{-1}. The present observation reveals the presence of surface cus K^+ ions, no longer screened by either sulfates of OH groups.

The concentration of cus K^+ ions on TSZ_{1073} samples, as revealed by the 8a band of $(py-L)_K$ at ≈1588 cm^{-1}, increases after vacuum activation at $T > 300$ K. This is most likely due to the dehydration of the K^+ centers and, at $T \geq 800$ K (curves b and c in Figure 6B), to the decomposition of the last surface sulfates which, on samples fired at high temperatures, were shown in Figure 3 to be mainly of the K-related type.

Still, on TSZ fired at $T < 1073$ K, the surface dehydration and the decomposition of sulfates did not yield any appreciable amount of cus K^+ centers to be revealed by $(py-L)_K$. In fact no such species can be observed in curve c of Figure 6A. This indicates that the liberation of K^+ canters at the surface of those materials either did not yield a sufficient concentration for the $(py-L)_K$ species to be detected (the surface area of those samples is still quite high) or was followed by the sinking of (most of) the K ions into the bulk of the particles.

Opposite to it, on samples fired at high temperatures (which possess low surface area), the surface concentration of K^+ may become high enough for the $(py-L)_K$ species to be detected and/or a segregation process of K ions from the bulk of the particles towards the surface may occur, as postulated elsewhere.[13] It was also suggested[13] that the segregation process may be made easier by the beginning of the anatase–rutile phase transition which, in the presence of rutile seeds, starts at $T \approx 1000$ K.

3.2. Thermal Treatments at $T > 1073$ K. The narrow interval of firing temperature 1073–1185 K, which leads to the so-called "final product", sintered pigmentary materials ready for the last operations (leaching and coating, to be dealt with in a following note), will be examined in detail only for the TSZ preparation, which we have already described in detail up to 1073 K.

A comparison between TSZ and the other preparations (TSK, TSA) will be limited to the final products, i.e., to the specimens in the final sintering stage, which each of them reached gradually in the mentioned temperature interval.

3.2.1. Effect of the Thermal Treatments (Background Spectra). Figure 8A shows, in the mid-IR range, the evolution of the spectrum of TSZ in the firing temperature interval 1073–1185 K, and the effect produced, on the spectrum of TSZ_T, by the adsorption of py. The following can be seen:

(i) With temperature, the scattering profile is severely modified, while the transparency to the IR radiation and the adsorptivity (the latter is revealed by the intensity of the py bands) decline dramatically, as expected of a powdery material whose surface area varies from ≈24 to ≈8 m^2 g^{-1}.

(ii) In $TSZ_{1073}673$ there is still a fair amount of surface sulfates (both of the Ti- and K-related type, and indicated in curves a by the upward arrow). Their ν_{SO} modes are appreciably shifted by py uptake. On $TSZ_{1073}873$ (curves b) all sulfates have been eliminated by the vacuum treatment at high temperature (as indicated by the downward arrow), and no apprecible spectral differences are observed in respect of a pure TiO_2 sample (e.g., see curve e of Figure 2);

(iii) On TSZ samples fired at $T \geq 1125$ K (curves c–e, Figure 8A) there is a weak spectral component at ≈1280 cm^{-1} (see the arrow pointing to curve c), whose intensity declines with firing temperature, and which is due to a surface species, as it is shifted by py adsorption (see the differential spectrum (c′ − c)).

It is not quite clear if that band is due to a residual amount of K-related sulfates, whose ν_{SO} mode has been further decreased at high temperatures, or to any other surface species produced during the high-temperature treatment. Elemental analysis data[13] confirm that, on these materials, some 0.1–0.3% S is still present, and XPS data indicate that the residual S is mainly located in the outermost layers. For a material of low surface area this may mean an appreciable amount in terms of surface coverage. On the other hand, IR data relative to the adsorption of py (see next section) exclude most of the spectral features reported in the previous sections as typical of the presence, on TSZ_T samples, of surface sulfates.

(iv) In the spectra of TSZ fired at $T \geq 1125$ K (curves c–e of Figure 8A) there is also a broad and complex spectral component centered at ≈1150 cm^{-1}, whose intensity declines with further increase of the sintering temperature (curves d and e) and which is not appreciably perturbed by py adsorption. This band is not peculiar to the TiO_2 phase, as no such a band is ever observed on pure TiO_2 treated at high temperatures, and must be somehow related to species at (or accessible from) the surface, as neutral or acidic leaching removes that band entirely (data to be reported in a forthcoming note).

Figure 8B shows that also the other TiO_2 pigmentary preparations considered in this work (TSA, TSK) possess, in the 1300–1000-cm^{-1} range, bands of variable shape and intensity. Some components of these bands are certainly related to surface species, as they are shifted upon py uptake (e.g., see the sharp band at ≈1230 cm^{-1} in the spectra of the TSA_T samples, curves b–d, and marked with the arrow), whereas some other components are not perturbed by surface interactions.

All of the bands observed on the various materials in the 1300–1000-cm^{-1} range are not observed when firing at 1080–1200 K either pure TiO_2 samples (TSS, TS), or samples of TiO_2 containing only one of the following ad-

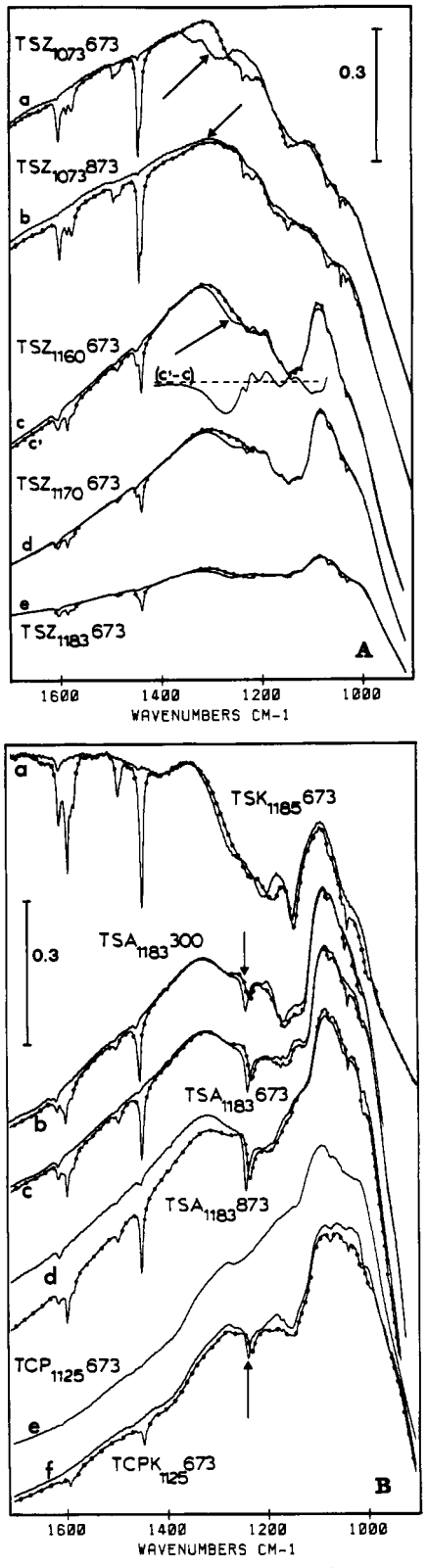

Figure 8. A: IR spectra in the 1700–900-cm^{-1} range of some TSZ_T samples, after vacuum activation (solid line curves) and after contact with ≈6 Torr of py (dotted line curves). (a) $TSZ_{1073}673$; (b) $TSZ_{1073}873$; (c) $TSZ_{1160}673$; (c'–c) absorbance differential segment of the spectrum of $TSZ_{1160}673$ before and after py uptake; (d) $TSZ_{1170}673$; (e) $TSZ_{1183}673$ (transmittance vs wavenumbers). B: IR spectra in the 1700–900-cm^{-1} range of some TSK_T, TSA_T, and some reference related samples, after vacuum activation (solid line curves) and after contact with ≈6 Torr of py (dotted line curves). (a) $TSK_{1185}673$; (b–d) TSA_{1183} vacuum activated at 300, 673, and 873 K, respectively; (e) the reference sample $TCP_{1125}673$; (f) the reference sample $TCPK_{1125}673$ (transmittance vs wavenumbers).

ditives: Kn, Zn, Al, P_2O_5 (e.g., see the reference spectrum e of $TCP_{1125}673$ in Figure 8B). On the contrary, bands of variable intensity and shape, comparable to those shown in Figure 8, are observed when firing at 1080–1200 K TiO_2 preparations containing P_2O_5 and other elements, such as K, which tend to segregate at the surface in the late stages of the sintering process. (Curve f in figure 8B shows the spectrum of the reference $TCPK_{1125}673$, in which a sharp band at ≈1230 cm^{-1} is particularly evident.)

It is thus deduced that on preparations such as TSZ, TSA, and TSK bands at 1300–1000 cm^{-1}, with the only exception being a component at ≈1280 cm^{-1} possibly ascribable to some residual surface sulfates, are generically ascribable to the presence of surface-accumulated cationic additives and of some P, deriving from the addition to the starting gel of some P_2O_5.

The proposed assignment is consistent with the spectral features reported in the literature for inorganic phosphates (e.g., see refs 27, 34, and 35) and with XPS data[13] that suggested that P tends to segregate at the surface of the TiO_2 granules in the late stages of the sintering process.

The actual nature and structure of the surface P-containing species, most likely phosphates, is not known and of a rather limited interest. In fact these species seem to interfere very little with the surface Lewis acidic behavior of the TiO_2 pigmentary preparations (see also the next section) and are eliminated during the leaching treatments.

It is here recalled that P_2O_5 is added to all TiO_2 pigmentary preparations to control the crystal growth and phase transition during the last firing stages. The present results suggest that this role is most likely played by P_2O_5 by modifying the anionic termination of the sintering TiO_2 crystallites.

3.2.2. Adsorption of Py. A. Some Features of the Py Spectra. (i) Py spectral range: In the figures of this section the region of the 19a band is omitted, as the weakness of that mode (in the absence of Brønsted py species) makes it of very little analytical use, whereas the possibility of using in the figures a more expanded abscissa scale for the other bands was thought to be preferable.

(ii) Py band subtraction: Some of the py spectra in Figures 4 and 6B showed that, for an adequate spectroscopic observation of all chemisorbed py species, the use of spectra run in the presence of a py pressure is often required. In fact not always is chemisorption a synonym of nonreversible adsorption.

Unavoidably, the spectra run in the presence of a py pressure also contain variable contributions from nonchemisorbed species, among which a liquidlike physisorbed phase (py–ph), whose absorptions may alter the profile and intensity of the bands of chemisorbed species.

For these reasons some of the spectra reported in this section are those obtained after sample equilibration with (≈6 Torr) py, thus possessing all chemisorbed species at their virtually maximum intensity, "cleaned" in the 8a–8b spectral region (1630–1550 cm^{-1}) from the spectral components due to the liquidlike phase. This was carried out through an interactive band subtraction procedure, described and tested elsewhere.[36] Examples of the spectral differences observable in the 8a–8b modes range before and after (py–ph) band subtraction are given in Figures 9 and 10, curves b (dotted and solid lines).

B. Py Adsorption and Surface Acidity. Py/TSZ system: Figure 9 reports the 8a–8b and the 19b region of py adsorbed on some TSZ and related samples.

(34) Chapman, A. C.; Thirlwell, L. E. *Spectrochim. Acta* **1964**, *20*, 937.
(35) Corbridge, D. E. C.; Lowe, E. J. *J. Chem. Soc.* **1954**, 493.
(36) Morterra, C.; Cerrato, G. *Langmuir*, in press.

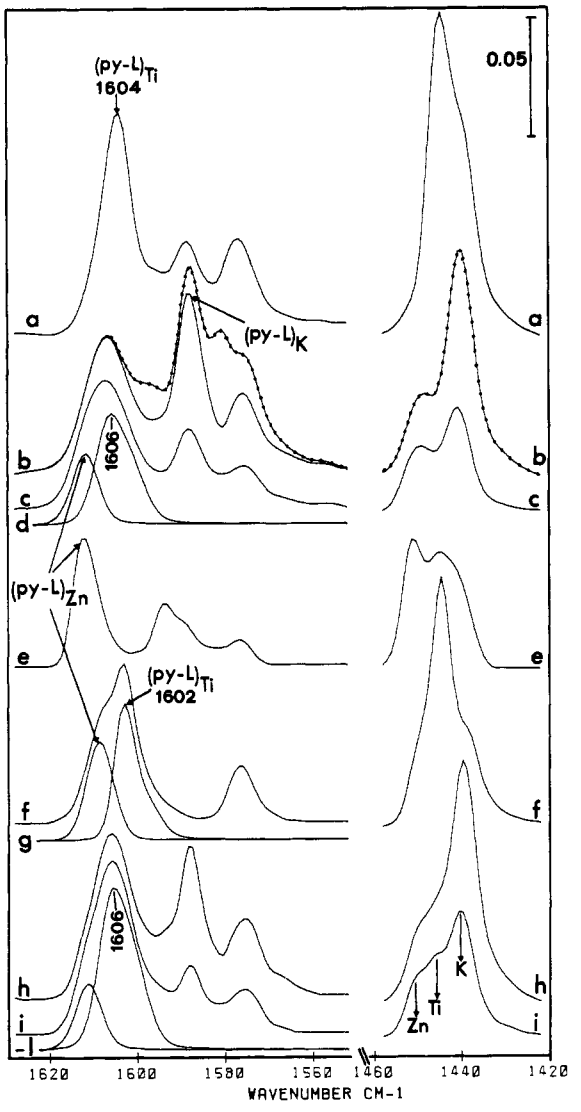

Figure 9. IR spectra in the 1630–1550- and 1460–1420-cm^{-1} ranges relative to the adsorption/desorption of py on some TSZ samples fired at $T \geq 1073$ K and on some reference related samples. (a) $TSZ_{1073}673$ equilibrated with ≈6 Torr of py, and band subtracted of the spectral contribution from (py–ph), the physisorbed liquidlike py phase; (b) $TSZ_{1160}673$ equilibrated with ≈6 Torr of py, before (dotted line) and after (solid line) band subtraction of the (py–ph) phase; (c) the $TSZ_{1160}673$ sample of curve b after py evacuation at ambient temperature; (d) band-resolved 8a mode components in the high-frequency range of the spectrum of curve c; (e) spectrum of the reference sample ZnO 698, after py adsorption and evacuation at ambient temperature; (f) spectrum of the reference sample TCZ 673, after py adsorption and evacuation at ambient temperature. In the high-frequency range, also the band-resolved 8a mode components of spectrum f are shown as curves g; (h) $TSZ_{1185}673$ equilibrated with ≈6 Torr of py, and band subtracted of the spectral contributions from (py–ph); (i) the $TSZ_{1185}673$ sample of curve h after py evacuation at ambient temperature. In the high-frequency range, also the band-resolved 8a mode components of spectrum i are shown as curves l (absorbance units vs wavenumbers).

Curve a corresponds to py uptake on $TSZ_{1073}673$ (i.e., on the sample of curves a of Figure 8A). Despite the residual presence of some surface sulfates, evidenced in Figure 8A, there is no (py–B) activity. The 8a mode of $(py–L)_{Ti}$ is at 1604 cm^{-1}, whereas after complete sulfate decomposition that mode is observed at 1602 cm^{-1} (see curve c of Figure 6B). These are small reproducible spectral shifts, which yield information on the side effects (adsorbate–adsorbate and/or inductive effects) acting on a surface.

Curves b and c correspond to the adsorption/desorption of py on $TSZ_{1160}673$ (i.e., on the sample of curves c–c′ of Figure 8A). A small increment of firing temperature did produce appreciable changes in the termination of the material, and the changes are monitored by py adsorption.

In fact the following can be noted:

(i) The segregation of K ions from the bulk to the surface of the particles has proceeded to a fair extent. This is revealed by the intensity of the 8a band at ≈1588 cm^{-1} and of the 19b band at ≈1440 cm^{-1} due to $(py–L)_K$. The fraction of the $(py–L)_K$ species that resists a short evacuation at ambient temperature (curve c) is only ≈20% of the amount adsorbed under a pressure of ≈6 Torr of py (curve b).

(ii) The 8a py band at $\tilde{\nu} > 1600$ cm^{-1}, due to the Lewis coordination to strong acidic centers, shifted upward and became broad and asymmetric on the high-wavenumber side, and so did the corresponding 19b component at ≈ 1450 cm^{-1}.

Trace d, showing the band-resolved 8a mode components in curve c, indicates that the band due to strong Lewis coordinated py is actually double, a new component being now present at ≈1611 cm^{-1}, in addition to the usual $(py–L)_{Ti}$ species. Its intensity accounts for ≈25–30% of the total 8a band at $\tilde{\nu} > 1600$ cm^{-1}.

Curves e and f of Figure 9, relative to the adsorption/desorption of py on ZnO (pure ZnO) and on TCZ (TiO_2 impregnated with Zn^{2+}) suggest that the new high-$\tilde{\nu}$ component is ascribable to the Lewis coordination of py to (tetrahedrally coordinated) surface Zn^{2+} ions. This species is hereafter referred to in the text and figures as $(py–L)_{Zn}$. Its analytical modes in the 1700–1400-cm^{-1} range are 8a, ≈1611; 8b, 1576, within the envelope of all the 8b modes of adsorbed py; 19a (not shown in the figure), ≈1488; 19b, ≈1452 cm^{-1}.

It is also confirmed that Zn, added to some of the TiO_2 preparations to play a photostabilizing role in the final pigment, tends to segregate at the surface of the crystallites only in the late stages of the sintering process, after the virtually complete elimination of sulfate contaminants and, possibly, in the presence of an early anatase–rutile phase transition.

It is as well deduced that Zn ions, when at the surface, can acquire easily a cus configuration. Py coordinates at these centers, yielding a strong Lewis acid–base surface complex, characterized by peculiar and easily recognizable spectral features.

(iii) The resolved spectral components of curve c, shown as curve d, show that the 8a mode of $(py–L)_{Ti}$ is here located at 1606 cm^{-1}, i.e., some 4 cm^{-1} higher than on sulfate-free TiO_2 and some 2 cm^{-1} higher than on the TSZ_{1073} sample of curve a.

The weak band at ≈1280 cm^{-1} discussed in the previous section, provided it is due to residual surface sulfates, cannot be solely responsible for an upward shift of the 8a band of $(py–L)_{Ti}$ larger than in the case of a sample richer in sulfates, as is TSZ_{1073}.

Other anionic structures must thus be present at the surface of these materials and produce, by inductive effects, a blue spectral shift of the 8a mode of the charge-releasing py species. These may be the surface phosphates, responsible for the complex absorption observed in the 1300–1000-cm^{-1} range of the background spectra reported in Figure 8A. This hypothesis is confirmed by the downard shift undergone, upon py adsorption, by some components of the complex band in the 1300–1000-cm^{-1} range, indicating a mutual perturbation between phosphates and py adspecies.

The last curves of Figure 9 (h–l) are relative to py adsorption on $TSZ_{1185}673$ (i.e., on the final TSZ product, shown by curves e in Figure 8A). The 8a mode of $(py–L)_{Ti}$ is still at ≈1606 cm^{-1}, confirming the inductive effect from phosphates postulated above. Besides, some further changes have occurred in the 1060–1185 K interval, which mainly concern the relative amounts of the various (py–L) species. If the 8b mode band at ≈1575 cm^{-1}, common to all Lewis coordinated species, is set in curves b and h at the same intensity, which corresponds to having, at maximum py coverage, the same overall amount of Lewis coordinated species, it turns out that the $(py–L)_{Zn}$ species is virtually unchanged in the two samples, whereas in the sample fired at higher temperature the $(py–L)_K$ component decreased and the $(py–L)_{Ti}$ increased appreciably.

This redistribution of the cationic termination of the particles occurred to such an extent that now also in the region of the 19b modes (≈1450 cm^{-1}) three distinct bands can be observed. They are due to three types of (py–L) coordination, as shown by the arrows in curve i, which involve a different degree of py N lone-pair charge donation to the coordinating center.

Py/TSK and py/TSA systems: Figure 10 summarizes some of the data relative to py adsorption on the TSK and TSA preparations.

Curve a refers to py on $TSK_{1073}673$. It is virtually identical with the corresponding $TSA_{1073}673$ (not shown) and is virtually indistinguishable also from the corresponding spectrum of $TSZ_{1073}673$, shown as curve a in Figure 9. This confirms that, up to the sintering stage represented by the firing at 1073 K, all TiO_2 preparations examined behave in the same way, no matter what additives they actually contain.

For firing at $T \geq 1125$ K, the behavior of TSK and TSA specimens differs appreciably from that of TSZ.

Curve b shows that the spectrum of py adsorbed at high coverage on the final TSK product possesses a preeminent band at ≈1588 cm^{-1}, ascribed to the 8a mode of $(py–L)_K$, to which corresponds a strong 19b band at ≈1440 cm^{-1}.

It is so deduced that the last stages of the sintering process of TSK led to the surface accumulation of a fair amount of K ions (much more than was observed in the case of TSZ). To that corresponds a much lower abundance of Ti ions in the uppermost layer, as revealed by the declined importance of the bands due to the $(py–L)_{Ti}$ adspecies. Note that the latter species is even less abundant than it may be suggested by the intensity of the band at ≈1604 cm^{-1}: in that spectral position occurs also the (1 + 6a) combination mode[17,31] of the most abundant $(py–L)_K$ species, so that the actual amount of $(py–L)_{Ti}$ must be thought to be fairly low. Consistently, its 19b mode at ≈1445 cm^{-1} (curves b and c) is hardly observed at all, but for a weak asymmetry on the high-$\tilde{\nu}$ side of the preeminent 19b band of $(py–L)_K$.

This means that the high-temperature sintering and the anatase–rutile phase transition of a material possessing some 0.18% K since the starting gel stage led to the production of a final pigmentary material whose surface layer is basically K titanate rather than TiO_2. The surface K ions readily acquire a cus configuration, yielding a Lewis coordinated py species, easily recognizable. The latter is (up to) 70% reversible for evacuation at ambient temperature (curves b and c).

In the case of the TSA specimens, the surface situation revealed by py adsorption and represented by the spectra shown as curves d–h in Figure 10 is somewhat less straightforward than in the case of TSZ and TSK. Schematically, the following can be observed:

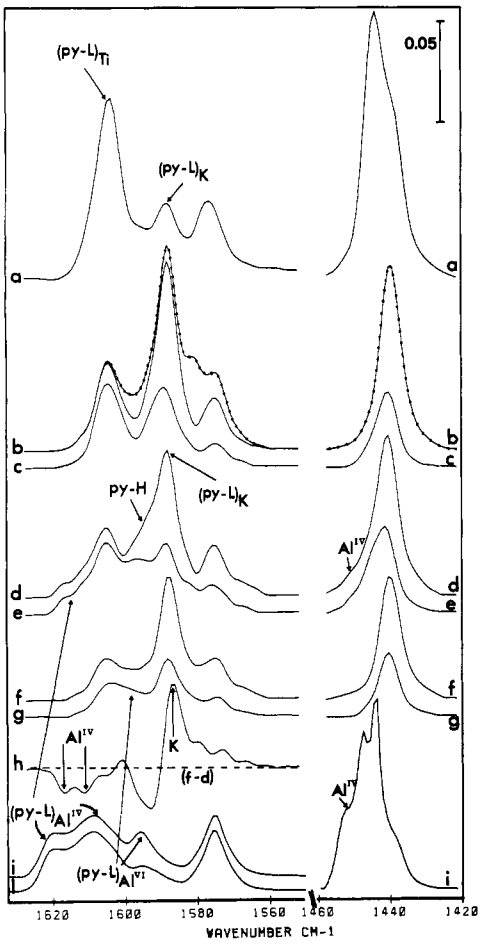

Figure 10. IR spectra in the 1630–1550- and 1460–1420-cm^{-1} ranges relative to the adsorption/desorption of py on some TSK and TSA samples fired at $T \geq 1073$ K, and on a reference related sample. (a) $TSK_{1073}673$ equilibrated with ≈6 Torr of py, and band subtracted of the spectral contribution from (py–ph), the physisorbed liquidlike py phase; (b) $TSK_{1185}673$ equilibrated with ≈6 Torr of py, before (dotted line) and after (solid line) band subtraction of the (py–ph) phase: (c) the $TSK_{1185}673$ sample of curve b, after py evacuation at ambient temperature; (d) $TSA_{1185}300$ equilibrated with ≈6 Torr of py, and band subtracted of the spectral contribution from (py–ph), the physisorbed liquid like py phase; (e) the $TSA_{1185}300$ sample of curve d after py evacuation at ambient temperature; (f) $TSA_{1185}873$ equilibrated with ≈6 Torr of py and band subtracted of the spectral contribution from (py–ph), the physisorbed liquidlike py phase; (g) the $TSA_{1185}873$ sample of curve f, after py evacuation at ambient temperature; (h) the differential spectrum (f–d). In (f–d), the negative bands (below the dotted line) correspond to species which decreased on going from d to f, whereas the positive bands (above the dotted line) correspond to species that increased on going from d to f; (i) spectrum of the reference sample $AlO(\theta)1000$ equilibrated with ≈6 Torr of py, and band subtracted of the spectral contribution from (py–ph), the physisorbed liquidlike py phase; (l) the $AlO(\theta)1000$ sample of curve i after py evacuation at ambient temperature (absorbance units vs wavenumbers).

(i) There is a prevailing abundance of the $(py–L)_K$ species (8a mode at ≈1588 cm^{-1}) relative to the $(py–L)_{Ti}$ species (8e mode at ≈1604 cm^{-1}). At high py coverage, the relative intensity of the two species is ≈2.5 on $TSA_{1185}300$ (curve d) and ≈4 on $TSA_{1185}873$ (curve f). In this respect the behavior of TSA (final product) is quite similar to that of TSK, whose surface layer contains more Ti in an anionic configuration (formally, a surface titanate) than in a cationic one.

(ii) On the $TSA_{1185}300$ sample the 8a mode region of adsorbed py (curves d–e) shows some additional contributions. There are two weak bands at $\tilde{\nu} > 1605$ cm^{-1} (≈

1617, ≈1612 cm^{-1}), indicating Lewis coordination to centers "harder" than cus Ti^{4+} ions. There is also a weak band at ≈1598 cm^{-1}, partly resisting evacuation at ambient temperature, indicating an adsorption weaker than the Lewis coordination to cus Ti^{4+} centers. The former bands are accompanied, as expected, by components at high wavenumbers also in the 19b mode region (≈1450 cm^{-1}). The band at ≈1598 cm^{-1} may be due to some py H-bonded to surface hydroxyls, and a perturbation of the ν_{OH} region (not shown in the figure) confirms it. Still, the persistence of that band after py evacuation at ambient temperature (curve e), and its presence also on TSA_{1185} samples activated at high temperatures and thoroughly dehydroxylated (see curves f and g) suggest that also a Lewis coordination to cus cationic centers "softer" than Ti^{4+} must be involved in that absorption.

The spectrum of curve i, inserted for comparison purposes, is that of py adsorbed on AlO(θ), a sample of θ-Al_2O_3 in which the surface layer presents the features typical of transition aluminas. In a previous work, dealing with the adsorption of py on α-Al_2O_3 and θ-Al_2O_3, that the reader is referred to,[37] we could ascribe the 8a py bands at $\tilde{\nu} >$ 1605 cm^{-1} to py Lewis coordinated to surface Al ions in a tetrahedral (θ) or quasi-tetrahedral (α) coordination [$(py\text{–}L)_A^{IV}$] and the band at $\tilde{\nu} <$ 1600 cm^{-1} to py Lewis coordinated to surface Al ions in a octahedral coordination [$(py\text{–}L)_{Al}^{VI}$]. The latter species obviously predominate at the surface of α-Al_2O_3, which possesses the corundum structure, whereas they are less abundant on transition aluminas in which the tetrahedral coordination is also present.

It is believed that the above assignment can be used to explain the py spectral features observed on $TSA_{1185}300$: for firing temperatures above ≈1073 K there is the surface segregation of some Al atoms in a form similar to that found on a transition alumina or on a defective α-Al_2O_3 phase.

The number of cus Al atoms, in both tetrahedral and octahedral coordination, revealed by py adsorption (curves d and e of Figure 10) is fairly small. This is particularly evident if one compares the low intensity of the Al-related py bands in Figure 10 with the intensity of Al-related bands one can observe in the case of a TiO_2 pigment coated with alumina.[38] This issue will be described in a forthcoming communication.

It is deduced that either the firing TSA at $T \geq 1100$ K and the anatase–rutile phase transition did not segregate much of the added Al from the bulk or the surface Al atoms were mostly involved in anionic rather than cationic configurations. The former suggestion agrees with the findings of a previous work,[13] in which XPS measurements could not reveal appreciable amounts of surface Al, so that a bulk retention of the Al atoms was postulated.

(iii) The py spectra obtained after vacuum activation of TSA_{1185} samples (see curves f and g and the differential spectrum h) show that the small amount of Al that was segregated at the surface in a cationic configuration, and especially the fraction exhibitng the (quasi)tetrahedral coordination (8a py modes at $\tilde{\nu} \geq 1610$ cm^{-1}), is unstable to the vacuum thermal treatments. In fact all of the high-$\tilde{\nu}$ bands in the 8a and 19b mode region, ascribed to $(py\text{–}L)_{Al}^{IV}$ species, are eliminated, as revealed by the negative bands marked with the arrows in the differential spectrum h. It is difficult to say whether the 8a band due to $(py\text{–}L)_{Al}^{VI}$ species decreased, because in that spectral position (≈1598 cm^{-1}) there is a strong negative band due to the obvious elimination of the py species H-bonded to surface hydroxyls.

Rehydration of the vacuum activated $TSA_{1185}873$ sample of curves f and g and subsequent adsorption of py showed that the H-bonded py species could be restored, as expected. Moreover, no evidence could be found anymore for the $(py\text{-}L)_{Al}^{IV}$ species, indicating that the thermal and vacuum instability of the latter species is independent of the hydration/dehydration degree. This most likely corresponds to a nonreversible modification in vacuo of the Al-containing surface structure(s).

4. Conclusions

The chemical/physical process proceeding from the starting (anatase) TiO_2 gel phases to the final (rutile) pigment is a rather complex one, in which at least two stages can be distinguished. First, an early one, due mainly to the progressive surface elimination of the impurities deriving from the via-sulfate preparative process, and a second one, in which the surface role played by the different additives becomes the main feature. The latter provides an element of differentiation among the various preparations.

In situ FTIR spectroscopy turns out to be particularly useful in following these complex processes, in that it can observe directly, step by step, what does change at the surface of the sintering materials.

In addition, the FTIR spectroscopic approach, as applied to surfaces progressively modified by thermal treatments and py adsorption, turns out to be of vital support to the preliminary understanding gained by the use of other techniques. These latter are quite powerful but not so specifically analytical of the surface layer.

The in situ FTIR technique applied to the study of thin-layer samples of low-area and highly scattering materials allowed us (i) to identify, at least in general terms, most of the surface structures produced in the various phases of the sintering process, (ii) to bring into evidence some small effects, of the adsorbate–adsorbate and/or charge withdrawing–charge releasing type, which cannot be observed by any other analytical tool (this casts some information on the structural and coordinative situation of the surface), and (iii) to identify the appearance (i.e., segregation) at the surface of various cationic additives, acting as Lewis acidic centers alternative to cus Ti^{4+}, and to postulate their relative abundance in respect of the regular TiO_2 network. The latter possibility, by far one of the most interesting, is made feasible by the systematic use of various coverage and/or activation conditions, as well as by the use of band subtraction and band deconvolution procedures.

Registry No. Py, 110-86-1; TiO_2, 13463-67-7; ZnO, 1314-13-2; Al_2O_3, 1344-28-1.

(37) Morterra, C.; Coluccia, S.; Chiorino, A.; Boccuzzi, F. *J. Catal.* **1978**, *54*, 348.

(38) Morterra, C.; et al., submitted for publication.